

# Phase offsets between core and conal components of radio pulsars and their emission altitudes

R.C.Kapoor\*

Indian Institute Of Astrophysics,  
Koramangala, Bangalore, 560 034, India

C. S. Shukre†

Raman Research Institute,  
Sadashivanagar, Bangalore, 560 080, India

October 25, 2018

---

\*email : rck@iiap.ernet.in

†email : shukre@rri.res.in

## Abstract

We present a new and a potentially powerful method for investigating emission altitudes of radio pulsar core and conal components by attributing them different altitudes. We provide a framework for a systematic understanding of resulting longitude offsets between them which are frequently observed. By investigating the contributions to these offsets due to aberration and the magnetic field line sweepback, we show that they are always dominated by aberration for all emission altitudes and inclination angles. This directly leads to the conclusion that the core emission does not necessarily come from the surface. Based on our results, the trends seen in the observational phase offsets imply that for a large number of pulsars the emission altitudes of core and conal components are close when compared to the light cylinder radius but not necessarily relative to the stellar radius. The altitude difference between core and conal components that we find are typically larger than the individual altitudes ascribed to them so far. Our results also allow very widely different but related core/cone altitudes. We find that data supports also this circumstance for some pulsars, which suggests a novel and natural explanation of the precursors in the Crab and similar pulsars. The pre- and post-cursor nature of these components arises because of large offsets caused by correspondingly large differences in the core and conal emission altitudes. We also show that the question of emission altitudes can not be divorced from considerations of the core/cone components' filling factors of the polar flux tube. We propose an empirical '1/3 rule' to concisely describe the observed core/cone morphologies. Combined with the core/cone phase offsets it allows a glimpse into the variation of these filling factors with altitude. Lastly, we outline how the full predictive potential of our results can be realised by combining them with a detailed analysis of the polarization and multifrequency observations.

## 1 Introduction

Knowledge of the emission altitudes of radio pulses is of great importance for an understanding of the pulsar emission physics. Various methods for estimating emission altitudes have been used in the past (for a review see Cordes, 1992). These methods have been applied in Rankin (1990, 1993), Phillips (1992), and also by Nowakowski (1994), Kijak and Gil (1998), Gangadhara and Gupta (2001), and Mitra and Rankin (2001), to derive altitudes for many pulsars. The latest method by Blaskiewicz et al. (1991) (henceforth BCW) proposed and utilised a novel offset between centroids of the pulse intensity profile and the linear polarization position angle curve, which would result due to aberration. Recently this method has been further used by von Hoensbroech and Xilouris (1997) (henceforth HX). However, a consensus on and an order in derived emission altitudes has not emerged. Here we propose another independent method to gain knowledge of altitudes of core and conal components, by attributing the

observed phase offsets between them to different altitudes.

The pioneering and sustained study of Rankin (Rankin 1983, 1990, 1993 hereafter respectively R1, R4, and R6) has established that the mean pulse profiles of radio pulsars often consist of components designated as core and conal having differing characteristics. On the basis of a large body of data concerning the pulse widths, it has been suggested that the core emission emanates from the full polar cap at an altitude  $r_{core}$  which is the same as the stellar radius,  $R_*$  (usually taken as 10 km) (R4). The conal emission is inferred to come from a hollow cone at an altitude,  $r_{cone}$ , of about 10-20  $R_*$  (R6). This was the first instance when different emission altitudes were attributed to different pulse components. About the values of altitudes there is no unanimity at present (Kijak and Gil 1998), but it is clear that core and conal emission altitudes could generally be different. Keeping in view the previously quoted emission altitudes of upto  $200R_*$ , we take for them a general maximum figure of the order of 20% of the light cylinder radius  $r_L = (cP/2\pi)$ , although the altitudes could vary with the pulsar period  $P$ , the inclination angle between the magnetic and rotation axes  $\alpha$ , and the fraction of the emission cap that is active. However, later we also comment on the possibility of having arbitrarily large emission altitudes.

It is obvious that components of pulsar radiation which emanate from different altitudes will show some differences in properties related to their emission altitudes. One such is the often seen non-coincidence of centres of the core components and mid-points of the conal pairs. This phase offset between core and conal components through kinematic effects provides a new method to learn about these emission altitudes. As we demonstrate later, it is unencumbered by the ignorance of details of the emission mechanism and allows interpretation of observations in more detail so as to constrain the theory.

What follows is a framework for a systematic understanding of these phase offsets between core and conal components as being due to their differing altitudes. This approach has many advantages because one can learn about emission altitudes by focussing on *different* pulse components observed at *one* frequency rather than studying *one* component at *different* frequencies. Firstly this complements multifrequency considerations (Philips, 1992; Kijak and Gil, 1998). More importantly it allows us to skirt the complications arising from our ignorance of radius to frequency mapping and related time delays etc. (Cordes 1992). Furthermore, we expect that our study will clarify whether the phase offsets are as expected from only the contributions we are considering or call for additional contributions which provide us with hints about the details of the emission process. Lastly let us mention that core emission coming from the stellar surface has implications for the pulsar matter's equation of state leading to strong indications that pulsars are strange stars rather than neutron stars (Kapoor and Shukre 1999, 2001). This makes it very important to verify if core components truly emanate on the stellar surface. This interpretation of the remarkable pulse width relation of Rankin rests crucially on the assumption that core emission comes from the *full* polar cap (R4). We shall see what implications

this has for the core/cone offsets.

In the relation between the emission altitudes of core/cone components and the phase offsets due to these differing altitudes, one inevitable kinematical contribution is due to differential aberration (Kapoor and Shukre 1998 hereafter KS). Another contribution would be due to the magnetic field line sweepback (henceforth *mfs*), first considered by Shitov(1983, 1985). Although these two have been considered previously, most often separately, we here combine them properly for the first time, while keeping in mind the core/cone distinction. In addition to these two there would be dynamical contributions related to details of the emission process which are at present not known. Ignoring these latter contributions, we investigate what the geometrical considerations of pulsar beams as delineated by the open field line structure of an oblique dipole rotator can tell us about these longitude offsets and their relation to the locations of the core and conal emission regions in the context of the polar cap model of pulsar emission.

For this purpose we adapt the general formulae of KS to the present situation. We then combine these with *mfs* results of Shitov. A net phase offset is then derived in the next section. Thus we treat aberration exactly and *mfs* in its presently available approximate form. Section 3 describes the behaviour of calculated offsets as the emission altitude is varied. Section 4 gives a comparison of the trends in the emission altitudes emerging from our results and observations, especially those which hitherto appeared puzzling. The consistency of our results with other altitude determinations is discussed in section 5 where we also bring in a new empirical '1/3 rule' to relate core/cone pulse widths and show the importance of the polar flux tube filling factors for these considerations. Conclusions and directions for future work which can exploit the full potential of this work are in section 6.

## 2 The core-cone phase offset

In many pulsars, it is seen that the core component is shifted relative to the center of the conal pair. We call this offset in terms of arrival time, a 'lead' or a 'lag', depending on whether the core component is placed earlier or later in comparison with the conal centre. Both cases are seen (typical offsets  $\simeq \pm 2^\circ$ ). As mentioned above the most direct explanation for these shifts is a combination of contributions from differential aberration and the *mfs*. At all altitudes, the contribution of toroidal component of the magnetic field of a pulsar works in a sense opposite to that of aberration. Aberration tries to cause the arrival times to be earlier compared to the case when aberration is ignored. Similarly the *mfs* tends to delay the arrival. A consistent treatment should include both simultaneously. and accordingly we calculate here the net phase offset of a pulse component centre.

## 2.1 The aberration offset

In KS we have considered the kinematical effects including aberration on pulsar beams in the polar cap model, and those fomulae we adapt to the present context. Using the same formalism and notation as in KS, we use two co-ordinate systems, one with the rotation axis as the  $z$ -axis (unprimed co-ordinates) and the other in which the magnetic axis is the  $z'$ -axis (primed co-ordinates). The magnetic dipole lies in the  $y - z$  plane at an angle  $\alpha$  to the rotation axis.

An emission point will have co-ordinates  $(r, \theta_e, \varphi_e)$  where  $r$  is the emission altitude. The radiation is supposed to be emitted in a direction  $(\theta_r, \varphi_r)$  tangent to the magnetic field lines. The latter is obtained by appropriately correcting  $(\theta_e, \varphi_e)$  for the tangential direction at any given point (the usual  $\frac{3}{2}$  factor for small  $\theta_e$ ). The polar cap boundary is defined by the locus of those angles  $(\theta_{eb}, \varphi_{eb})$  which describe the feet of last open field lines. Therefore, the emission can emanate from the emission cap whose boundary is defined by the corresponding angles  $(\theta_{rb}, \varphi_{rb})$ . As shown in KS the effects due to the stellar gravitational field namely change in the dipole geometry and light bending are mutually opposite and leave the Goldreich-Julian (1969) type of beam essentially unaltered. These effects rapidly become insignificant for altitudes beyond a few stellar radii. More importantly they affect the emission cap in a symmetrical way through an overall shrinking. We therefore ignore these general relativistic effects here. The directions  $(\theta, \varphi)$  after aberration are denoted by angles  $(\hat{\theta}, \hat{\varphi})$ . The aberrated values  $(\hat{\theta}_r, \hat{\varphi}_r)$  of the angles  $(\theta_r, \varphi_r)$  are given by (KS - Eqs. 37 and 38),

$$\cos \hat{\theta}_r = \frac{\cos \theta_r}{\gamma[1 + v \sin \theta_r \sin(\varphi_r - \varphi_e)]}, \quad (1)$$

and

$$\tan(\hat{\varphi}_r - \varphi_e) = \frac{\gamma[\sin \theta_r \sin(\varphi_r - \varphi_e) + v]}{\sin \theta_r \cos(\varphi_r - \varphi_e)}. \quad (2)$$

where  $\gamma = (1 - v^2)^{-1/2}$  is the Lorentz factor and with

$$\xi = r/r_L, \quad v = \xi \sin \theta_e \quad (3)$$

is the corotation velocity of the emission point at altitude  $r$  and  $r_L$  is the light cylinder radius.

One can transform the  $\hat{\theta}_r$  and  $\hat{\varphi}_r$  values to the magnetic coordinates through

$$\sin \hat{\theta}'_r \cos \hat{\varphi}'_r = \sin \hat{\theta}_r \cos \hat{\varphi}_r, \quad (4)$$

$$\sin \hat{\theta}'_r \sin \hat{\varphi}'_r = \sin \hat{\theta}_r \sin \hat{\varphi}_r \cos \alpha - \cos \hat{\theta}_r \sin \alpha, \quad (5)$$

$$\cos \hat{\theta}'_r = \cos \hat{\theta}_r \cos \alpha + \sin \hat{\theta}_r \sin \hat{\varphi}_r \sin \alpha. \quad (6)$$

The pulses will be observed by us when the direction  $(\hat{\theta}_r, \hat{\varphi}_r)$  coincides with our line of sight. If the direction of line of sight is specified by angles  $(\theta_{LS}, \varphi_{LS})$  then the sweep of the line of sight through the emission cap is given by

$$\hat{\theta}_r = \theta_{LS} \quad \hat{\varphi}_r = \varphi_{LS} \quad (7)$$

where the angle  $\hat{\varphi}_r$  will change by an amount  $\Omega t$  in time interval  $t$  but  $\hat{\theta}_r$  remains constant. Here  $\Omega$  is the pulsar angular velocity.

Values of  $\hat{\theta}_r$  and  $\hat{\varphi}_r$  are larger than those of the unaberrated angles  $\theta_r$  and  $\varphi_r$ . For the special case of points lying on the meridian including the rotational and magnetic axes the formulae are simpler. In this case we confine attention to the  $y - z$  plane, i.e.,  $\varphi_e = \varphi_r = \pi/2$ . Consequently,

$$\cos \hat{\theta}_r = \frac{\cos \theta_r}{\gamma}, \quad (8)$$

and

$$\tan(\hat{\varphi}_r - \frac{\pi}{2}) = \frac{\gamma v}{\sin \theta_r}, \quad (9)$$

After including aberration the impact angle  $\beta$  needs care in its definition. In absence of aberration the usual definition is  $\beta = \theta_r - \alpha$  where  $\varphi_r = \pi/2$  is understood. Now we can define it for example as  $\beta = \hat{\theta}_r - \alpha$  with  $\hat{\varphi}_r = \pi/2$  understood. The relation of  $\beta$  with the locations  $(\hat{\theta}_r, \hat{\varphi}_r)$  is then not simple. With the desired definition of  $\beta$ , its relation with  $\hat{\theta}_r$  and  $\hat{\varphi}_r$  can be derived using Eqs. 1 and 2 or Eqs. 8 and 9.

Henceforth, we consider the longitude offset only for the simple case of the direction of the magnetic axis. Firstly this should suffice for understanding the gross properties of the offsets which is our aim here, and secondly because the corresponding *mfs* offsets are available only for this case (Shitov 1983). Therefore, in addition to  $\varphi_e = \varphi_r = \pi/2$  we also have  $\theta_e = \theta_r = \alpha$ . Now  $v = \xi \sin \alpha$  and then

$$\cos \hat{\theta}_r = \frac{\cos \alpha}{\gamma}, \quad (10)$$

$$\tan(\hat{\varphi}_r - \frac{\pi}{2}) = \gamma \xi, \quad (11)$$

Eqs. 9 and 11, in the nonrelativistic limit reduce to the often used  $v/c$  formula.

The offset in longitude introduced by aberration is

$$\varphi_{ab} = \hat{\varphi}_r - \varphi_e = \hat{\varphi}_r - \frac{\pi}{2} = \gamma \xi, \quad (12)$$

## 2.2 The magnetic field line sweepback and the net offset

Equating the pulsar braking torque to the product of stellar magnetic moment and the toroidal component of the magnetic field caused by the stellar magnetic dipole radiation Shitov (1983, 1985) derived the toroidal magnetic field component  $B_t$  as

$$B_t = \frac{2\sqrt{\pi}}{3} B_0 (R_*/r_L)^3 \sin^2 \alpha \quad (13)$$

where  $B_0$  is the polar surface magnetic field. The magnitude of the magnetic field at a distance  $r$  is  $B(r)$ . Presence of  $B_t$  changes the azimuth of the co-rotating and radiating charges by an amount  $\varphi_{mfs}$  such that

$$\tan \varphi_{mfs} = \frac{B_t}{B(r)} = \frac{r^3 B_t}{R_*^3 B_0} = \frac{2\sqrt{\pi}}{3} \xi^3 \sin^2 \alpha \quad (14)$$

which depends on  $r = \xi r_L$  but not on  $B_0$ . (Shitov quotes and uses this in the small angle approximation).

Eq. 13 was derived with various simplifying assumptions. Here we use this result without any modifications. It should be kept in mind that a proper derivation of this equation should make use of the magnetic fields given by the full Deutsch solution (Deutsch 1955). In addition the toroidal component will also get a contribution from the stellar wind current which though unknown at present, still may be contributing to the pulsar slowdown (Goldreich and Julian 1969). Both these factors would warrant a much more involved analysis which is beyond the scope of this work. We intend to address these later. We also use Eq. 14 as if it were valid for all emission altitudes. Actually we expect that a more precise handling of the  $mfs$  would certainly modify or even radically alter this equation for high altitudes. Therefore caution is advised in using Eq. 14 for  $\xi \simeq 1$ . Similarly, it would be proper to correct the emission direction due to the  $mfs$  first and then aberrate it. This would give us the net phase offset  $\Delta\varphi$ . Due to the crude way in which we are including the  $mfs$  we here simply subtract the two contributions. This would be certainly adequate for low emission altitudes where both contributions are small. For higher altitudes we are assuming that the offsets though not precise will still be qualitatively correct. Thus, for any emission component,

$$\Delta\varphi(\xi) = \varphi_{ab} - \varphi_{mfs} \quad (15)$$

where  $\varphi_{ab} = \hat{\varphi}_r - \varphi_e$  is given by Eq. 11 and  $\varphi_{mfs}$  by Eq. 14.

We vary the emission point ( $\xi$ ) from the stellar surface to the light cylinder along the radial direction. As mentioned above we look at  $\Delta\varphi$  for the magnetic axis direction. It should be kept in mind that this gives a somewhat distorted picture of things because approximating the offset by that for the magnetic axis ignores the differential aberration over the emission cap which may be substantial at high altitudes.

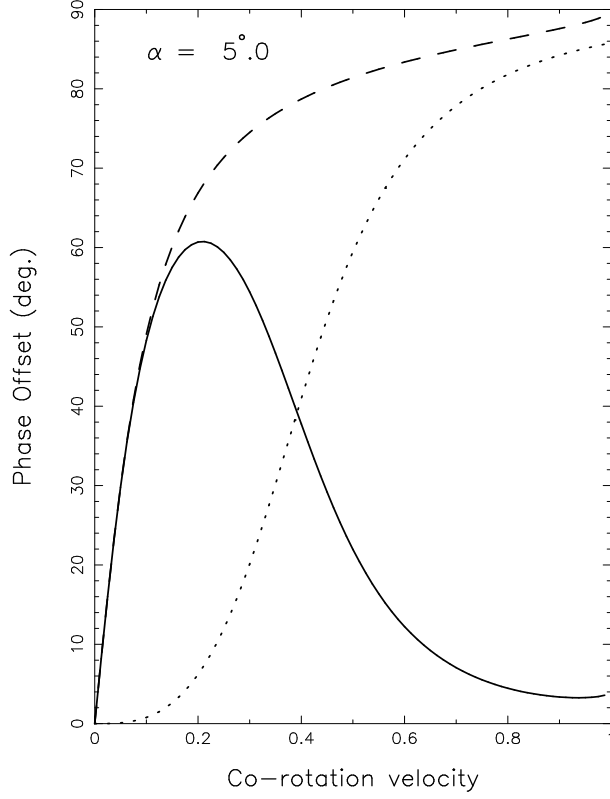


Figure 1: Phase offsets of the emission point as a function of corotation velocity for  $\alpha = 5^\circ$ . Dashed line is the contribution  $\varphi_{ab}$  due to aberration and dotted line is  $\varphi_{mfs}$  due to *mfs*. Solid line is the net offset  $\Delta\varphi(\xi)$  of Eq. 15.

Note that in the limit in which light cylinder is approached, i.e., as  $\xi \sin \alpha \rightarrow 1$ ,

$$\tan \varphi_{ab} \rightarrow \infty, \quad \text{i.e.,} \quad \varphi_{ab} \rightarrow \pi/2, \quad (16)$$

and,

$$\tan \varphi_{mfs} \rightarrow 1.18 \sin^2 \alpha. \quad (17)$$

If  $\alpha \simeq \pi/2$ ,  $\varphi_{mfs} \simeq 1 \text{ rad}$  and the net phase shift  $\Delta\varphi$  would be  $\simeq 0.57 \text{ rad}$ .

As is customary, we assume that narrow-band emission emanates from a given altitude. With  $r_{core}$  and  $r_{cone}$  as altitudes for core and conal components respectively, we denote the phase offset between the core peak and the conal center by  $\Delta_{cc}$  and it is given by,

$$\Delta_{cc} = \Delta\varphi(\xi_{core}) - \Delta\varphi(\xi_{cone}). \quad (18)$$

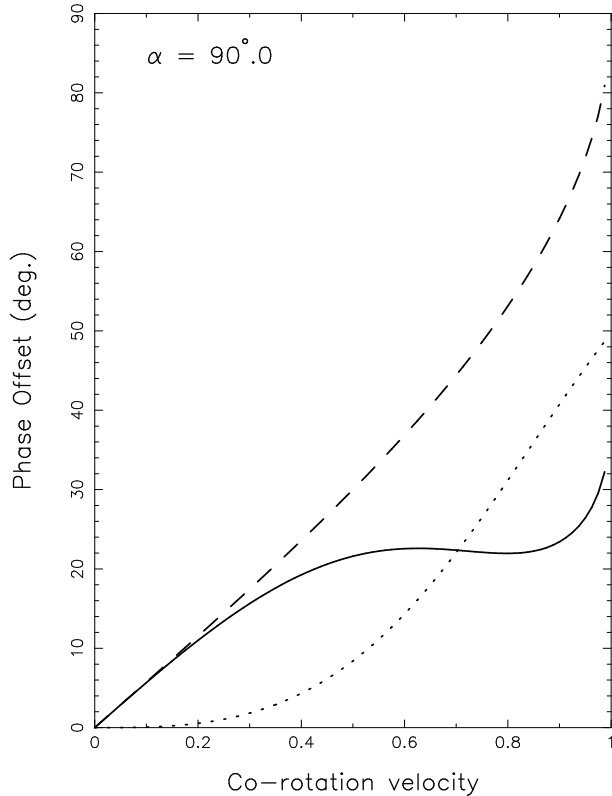


Figure 2: Same as Fig. 1 but for  $\alpha = 90^\circ$ .

In addition, we also define

$$\Delta r = |r_{core} - r_{cone}|, \quad (19)$$

$$\Delta v = |\xi_{core} - \xi_{cone}| \sin \alpha. \quad (20)$$

### 3 Calculated offsets

The latitude offsets (i.e.,  $\hat{\theta}_r - \theta_r$ ) though interesting can not be directly related to observations presently available. We therefore concentrate only on the longitude offsets  $\Delta\varphi$ . Using Eq. 15 we have calculated the offsets  $\Delta\varphi$  over the range of co-rotation velocity for various values of  $\alpha$ . Figs. 1-4 show these plots for  $\alpha$  values as labelled.

Figs. 1 and 2 show the individual contributions due to aberration and *mfs* and the net offsets in the small and large  $\alpha$  cases of  $5^\circ$  and  $90^\circ$ , while Figs. 3

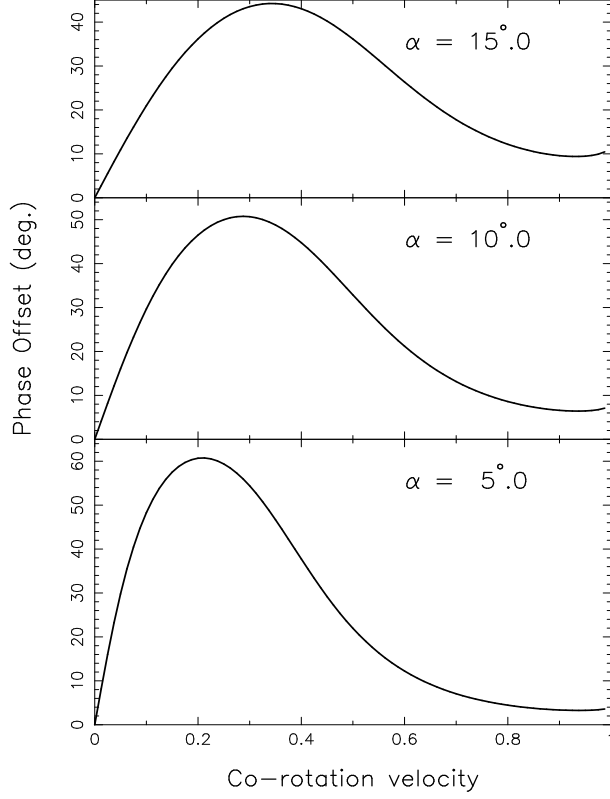


Figure 3: Net offsets  $\Delta\varphi$  vs. co-rotation velocity for various  $\alpha$  as labelled.

and 4 show the net offsets,  $\Delta\varphi$ , as a function of the co-rotation velocity of the emission point. Qualitatively, the plots share many common features.

Most notably the net offset is positive for all values of  $\alpha$  and co-rotation velocity  $v$ . *This means that aberration is always winning over mfs at all altitudes and inclination angles* as is evident from Figs. 3 and 4. The *mfs* contributes insignificantly until  $v$  increases to 0.2. The magnitude of *mfs* relative to aberration picks up for intermediate values of  $v$ , and the net offset is seen to vary in an interesting manner. For all  $\alpha$ ,  $\Delta\varphi$  has a peak whose location shifts to higher values of  $v$  as  $\alpha$  increases. The picture is more or less the same for all inclination angles above about  $20^\circ$ . The phase shift,  $\Delta\varphi$  first rises up to about half the distance to the light cylinder (we call this part of the curve as the rising branch) and then slopes down, rising again at  $v$  around  $0.8c$ . *The peak value of  $\Delta\varphi$  can be as large as  $60^\circ$  for  $\alpha = 5^\circ$ , decreasing to  $\cong 30^\circ$  for  $\alpha = 45^\circ$ .* For higher  $\alpha$  the maximum is attained at  $v = 1$ .

We see that for a given offset, the emission altitude is not uniquely deter-

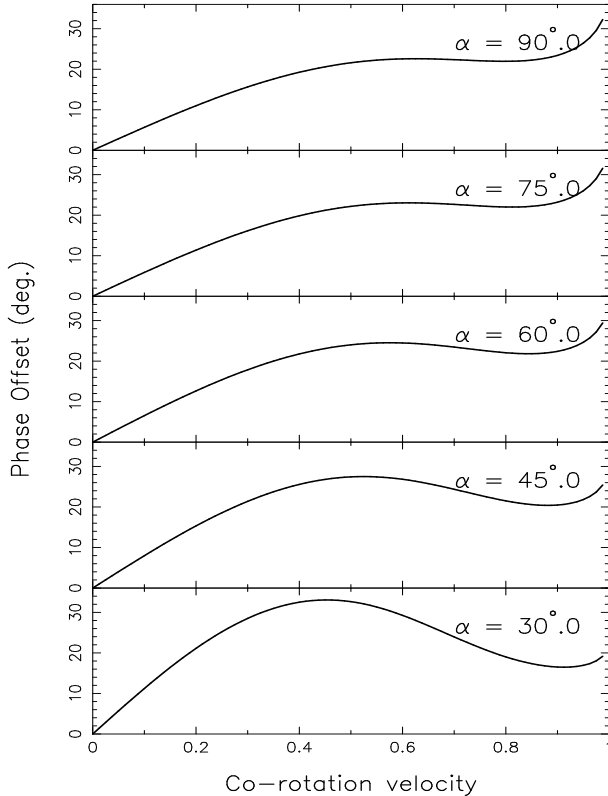


Figure 4: Same as Fig. 3 but for different  $\alpha$  values.

mined by  $\Delta\varphi$ . For  $\alpha \leq 60^\circ$ , the same  $\Delta\varphi$  is possible for two altitudes, while for  $\alpha \geq 60^\circ$ , a whole interval of altitudes is possible. Thus the altitude is a multivalued function of the offset  $\Delta\varphi$ .

It is worthwhile to keep in mind that our plots when applied to a specific pulsar select a particular range of the  $x$ -axis. This range is determined by both the period of the pulsar and the assumed emission altitude. Clearly, for a given emission altitude, the co-rotation velocity will increase inversely with the pulsar period.

Now we turn to the comparison of  $\Delta_{cc}$  with observations.

## 4 Comparison with observations

The core/cone phase offsets can constrain only the difference between the two emission altitudes. Therefore, it is not possible to make a direct comparison of

our results with observations so as to fit for individual pulsar parameters. This as will be seen would require that at least one of the core or conal emission altitudes is known. Still our results shed light on some important aspects of emission altitudes. Consequently, we focus on *trends* shown in observations rather than very precise agreements between them and the theory. For this purpose, although good and recent data is available with the European Pulsar Network maintained by MPI, Bonn (<http://www.mpifr-bonn.mpg.de/div/pulsar/data/>) we have used older pulse profiles which should suffice for our purpose. In our illustrative search we restricted to profiles from which offsets could be obtained by simple visual inspection, i.e., we typically searched for offsets among pulsars which are conal triples. We collected 59 triple (T) and multiple (M) profile pulsars (Lyne and Manchester 1988, henceforth LM88 and R4) where the star types are as defined in R4. Of these, useful profiles could be identified for 20 pulsars. The pulsars which show a leading core component are 4 in number, 6 show zero phase offset and 10 show a lagging core. (If M types are not included then these numbers are respectively 3, 6, and 7 out of a total of 16 stars of type T). Table 1 shows these pulsars and their characteristics. The phase offset values generally correspond to 400 MHz data from the references listed there. The star types,  $\alpha$  and  $\beta$  values, here as well as in Table 2 which comes later, are from R4 or LM88. They no doubt will have some inter-relation with  $\Delta_{cc}$ . Within the scope of this paper, we do not dwell on these details.

Although very large altitudes may come into play for emission from outer gaps (see Hirotani (2000) and references therein), from all indications so far it seems that usual pulsar emission altitudes are  $< 0.2 r_L$ . As noted before our inclusion of *mfs* also has limitations for very large altitudes. Therefore to avoid needless complexity we first concentrate on the rising branch of the  $\Delta\varphi$  curves in Figs. 3 and 4.

To derive a core/cone altitude difference all one needs is to assume appropriate altitudes for core and conal components, read off the corresponding offsets from the curve and compare their difference with the observed values. Values of  $\Delta r$  and  $\Delta v$  derived in this manner are included in Tables 1 and 2. Based on such a view of altitudes, explanation of offsets in Table 1 does not present any problem. In fact, the offsets probably are pointing towards some properties of emission altitudes.

#### 4.1 What do signs of observed offsets indicate ?

Assume that the core emission comes from the stellar surface as the simplest interpretation of the observed core widths (R4) : then, the corresponding  $\Delta\varphi$  for core is very small and almost same as that for  $v = 0$ . The conal emission must now come from a higher altitude (e.g.,  $10 - 20 R_*$  according to R6). It is obvious from the figures that if the offsets are attributed to the effects considered here then the core component can only lag. Observationally both cases are seen in Table 1. A majority of stars do show a lag, but the stars which do not conform

to this are not negligible ( about 50%). Our sample can not reliably tell what will be the actual fraction of such stars. But in all such cases clearly the core emission can not come from the surface. *The signs of observed offsets thus indicate that each of the possibilities, i.e.,  $r_{core} <, =, \text{ or } > r_{cone}$  can occur.*

## 4.2 What do magnitudes of observed offsets indicate ?

The magnitude of  $\Delta_{cc}$  in Table 1 generally is  $\cong 2^\circ$ . The first notable thing is its smallness compared to the maximum possible values seen in the Figs. 3 and 4 ( $\cong 30^\circ - 60^\circ$  depending on  $\alpha$  values). It is necessary to stress here that a small value of  $\Delta_{cc}$  which implies a small  $\Delta v$  will translate to a small  $\Delta r$  only for some values of  $\alpha$  and  $P$ , even when altitudes lie on the rising branch. *The magnitudes of  $\Delta_{cc}$  thus indicate that  $r_{core}$  and  $r_{cone}$  are closeby in comparison to  $r_L$  but not necessarily so in terms of  $R_*$ .*

As examples let us look at altitude differences for two pulsars in which the core lags. Using Eq. 18 for  $\Delta_{cc}$  we get an altitude difference for PSR 0329+54 as  $\Delta r \cong 115R_*$ , and for PSR 1913+16 as  $\cong 65R_*$ . We shall return in Section 5 to these values of  $\Delta r$  for lagging cores and the zero offset cases to see if they can be reconciled with altitudes derived in HX, R4 and R6. If on the other hand we consider two examples from pulsars in which the core leads, i.e., PSR 1917+00 and PSR 2028+22, then we get  $\Delta r$  as  $\cong 60R_*$  and  $\cong 100R_*$  respectively. In these pulsars the core altitude must be larger than the conal one, which is not possible with altitudes given in HX, R4 or R6.

## 4.3 Can both core and cone emission altitudes be very large ?

Although we are restricting to emission altitudes  $< 0.2r_L$ , if we consider altitudes  $> 0.2r_L$  a small  $\Delta_{cc}$  is still possible. The curves in Figs. 3 and 4 allow, in principle, widely different altitudes which lie on the opposite sides of the peak for smaller  $\alpha$ . Though widely different, these altitudes correspond to about the same small  $\Delta\varphi$  leading to even smaller  $\Delta_{cc}$ . For larger values of  $\alpha$  the peak in  $\Delta\varphi$  is not pronounced so a small value of  $\Delta_{cc}$  can occur for a larger range of  $\Delta r$  and the correlation that a larger lead corresponds to a larger altitude would not hold. As remarked earlier, our results warrant caution for high altitudes beyond the peak. There is one more caveat. For  $\xi > \frac{2}{3}$  the angular size of the emission cap exceeds  $180^\circ$ , and emission therefore must come from only a part of the cap. Without some further insights there is not much advantage in considering very large emission altitudes for both core and conal components especially when  $\Delta_{cc}$  is small. This notwithstanding, for larger values of  $\Delta_{cc}$  at least one of the altitudes must be very large. This case will be characterised by the core/cone altitudes being widely different. We discuss this in the next subsection.

#### 4.4 Can core and cone emission altitudes be widely different ? : Peculiar data

As for the very large values of  $\Delta\varphi$  which are seen in our plots, do they really manifest in some pulsars? If so then some interesting possibilities emerge.

One possibility is that a large offset makes the core component merge with one of the conal ones. The core then would seem absent or barely discernible. The conal pair in that case will not display symmetrical intensity and polarization, and typical spectral properties. In some triples, i.e., of type T, this may be a cause of confusion in their classification. One would expect this to be likely in those pulsars which have small  $\beta$  and absent or weak core component with conal components showing confusing characteristics. Observationally such a possibility was noted long ago but was not pursued as is demonstrated by the following quote, '...we must recognize the possibility of double profiles which are actually partially merged triples - particularly where there is a marked lack of symmetry between the two components in amplitude, width, or polarization behavior..' (R1 p. 343).

Another interesting possibility is that the offset is so large that the core may even be displaced outside the conal pair.

A search through observed profiles with this in mind led us to the stars listed in the Table 2. These cases are of great interest and may throw much light on pulsar emission altitudes. The longitude offsets quoted in the Table 2 as for Table 1 were read from published profiles and though not very precise, suffice for our purpose. For first eight stars, the  $\Delta_{cc}$  values equal one-half of the longitude separation between the two visible peaks, and are upper limits because the core/cone distinction is not completely clear in the profile. The star types are again as in R4.

The first eight stars in Table 2 illustrate the merging of the core component with one of the conal ones. The last four correspond to the core components being displaced outside the cone. We discuss them one by one.

1. PSR 1802+03 :

"The extremely high linear polarization and flat position angle of the leading component argue that it is a core or possibly a merged core and cone, with the trailing component being conal" (Weisberg et al. 1999). The core thus leads by  $\leq 4.1^\circ$ .

2. PSR 1822-09 :

This pulsar has been described variously as "most interesting" and "intriguing" (Manchester et al. 1980, Rankin 1986, hereafter R3) and is identified as a one-sided triple ( $T_{1/2}$ ). Its profile strikingly resembles that of the Crab pulsar (both exhibit interpulses). The main pulse profile is double with the leading component ("precursor") showing conal characteristics. The core component in this star is identified as the leading component of the composite second "component" of the main pulse (R6). From a 1612 MHz profile (Manchester et al. 1980; see also R3), we read the core component lag as  $7.5^\circ$ .

3. PSR 1842+14 :

Similar to PSR 1802+03 in 1 above (Weisberg et al. 1999) with core lead  $\leq 3.9^\circ$ .

4. PSR 1859+03 :

Profile is similar to PSRs 1802+03 and 1842+14 but core is identified here from its circular polarization signature (Weisberg et al. 1999), and lags by  $\leq 5.6^\circ$ .

5. PSR 1907+10 :

At 21 cm and higher frequencies, the leading component is apparently conal while the primary component is a core, possibly with another weak one merged on to its trailing edge (Weisberg et al. 1999). The core lag is  $\leq 3.8^\circ$ .

6. PSR 1920+21 :

In this star the core component is so early that it virtually overlies the leading conal outrider (R6; see also Rankin et al. 1989, hereafter RSW89). A 1418 MHz profile (Weisberg et al. 1999) gives the core lead as  $4.5^\circ$ .

7. PSR 2020+28

In the profile of this pulsar as seen in Sieber et al (1975) and Cordes et al (1978), the two conal components obscure the weak core component on the trailing edge of the leading component (R6) which also has been termed as a bridge (Weisberg et al. 1999). The profile can be modelled as the sum of three Gaussian components, in which the steep spectral index above 800 MHz of the bridge "suggests" that it is a core (Weisberg et al. 1999). From the profile at 430 MHz in Sieber et al. (1975), we find that the core leads by  $5^\circ$ .

8. PSR 2224+65 :

This pulsar is classified as a partial cone star in LM88, while according to R6 the profile has two well separated components of which the first seems to be the core component (steeper spectrum), which overlies the leading conal outrider. From a 1420 MHz profile in Seiradakis et al. (1995), we find that the core leads by  $15^\circ$ .

The next four pulsars show cores with offsets so large that they have been displaced outside the conal pair.

9. PSR 0531+21 :

The Crab pulsar though very well studied is not well understood. The precursor, "by virtue of its softer spectrum .... should probably be regarded as a core component" (R4). The precursor-main pulse profile is interpreted as a triple profile in which the leading conal outrider is missing (R6). Interpreted in this manner the core leads by  $22^\circ$  ( 318 MHz profile in McCulloch et al. 1976). Due to the  $T_{1/2}$  nature of the profile,  $\Delta_{cc}$  can not be determined unambiguously. We have taken the core lead as of the same order as the separation  $22^\circ$ . See the similar case of PSR 1055-52 discussed below.

10. PSR 0823+26 :

"The main pulse is readily identified as a core component (... circularly polarized signature), and the weak interpulse may be one also. The overall main pulse-postcursor complex might again be regarded as a  $T_{1/2}$  profile but

the 30° spacing is again rather large” (R4, see also RSW89). Again this seems to be a case where the core is leading by 30° (the 1400 MHz profile in RSW89).

Note the magnitude of  $\Delta_{cc}$  in this pulsar. With  $\alpha$  for this pulsar quoted as 90° the core emission occurs very close to the light cylinder (see Eqs. 16 and 17) if our *mfs* can be relied on. From our plots a 30° offset can be obtained at a lower altitude for a small  $\alpha$ . Therefore, both, a better treatment of *mfs* and a verification of the  $\alpha$  value would be of help.

#### 11. PSR 1055-52 :

The PSR 1055-52 shows great similarity to the Crab pulsar, though there are some minor differences. ”Clearly we should regard the main pulse as having a T profile” (R4). The interpulse and the precursors in both of these very strongly display properties typical of core components (McCulloch et al. 1976, R1). Thus, like PSR 0531+21 this pulsar is also an interesting example in which the core has been displaced outside the conal pair with a lead of 16° (the 635 MHz profile in McCulloch et al. 1976).

#### 12. PSR 1742-30 :

”The core component of this very interesting pulsar seems to follow the trailing 'outrider'- a very unusual configuration !” (R6). ”In pulsar 1742-30 we then seem to have either a five-component (M) profile with missing components 4 and 5 or a triple (T) profile in which the core component lies outside of the conal outriders !” (Xilouris et al 1991; see also Seiradakis et al. 1995). This is a case in which the core lags; we read it as amounting to 9° from a 1700 MHz profile in Xilouris et al. (1991).

*Table 2 thus clearly demonstrates that widely different core/cone altitudes, differing by a significant fraction of  $r_L$ , do occur in some pulsars.*

In the first three pulsars in this group, the nomenclature main pulse has been used in varied senses by different authors. But if the separation between similar components is considered the time lag comes much closer to half the pulsar period, in fact within the expected errors it may be exactly 180°. For the above pulsars the interpulse is core emission and therefore should be compared only with the core component of the non-interpulse. *We believe that the mystery of main pulse - interpulse separations being much different from the expected value of 180° may get completely solved if the data is reanalysed to obtain more precise values of  $\Delta_{cc}$  for these pulsars than what we have.* We hope to report on this soon.

## 5 Consistency with other altitude determinations

### 5.1 Consistency with the core width relation

The relation derived from observations by Rankin (R4) for core component widths besides being a very good fit to observations also lends itself to a very natural interpretation that the core emission originates from the stellar surface

and the full polar cap of a magnetic dipole. The polar cap (i.e., the emission cap on the stellar surface) size is the usual one for a dipole as given by Goldreich and Julian (1969). Recently we have analyzed this further after inclusion of general relativistic effects due to the stellar mass (Kapoor and Shukre 2001). The gravitational effects lead to constraints that  $M_{pulsar} < 2.5 M_{\odot}$  and  $R_{pulsar} \leq 10.5 \text{ km}$ . None of the available equations of state of the neutron star matter can satisfy the radius constraint for a reasonable mass, leading one to the conclusion that pulsars are strange stars rather than neutron stars. From the present work it appears that core emission may not originate from the stellar surface. Is it possible to choose between these two opposite views of core altitudes? Later in the section we show that assumptions needed for the usual interpretation of the Rankin core width relation need a revision, and therefore the constraints on pulsar radii would also get revised.

## 5.2 Consistency with pulse component widths

The altitude difference derived using  $\Delta_{cc}$  must be consistent with altitudes determined by other methods. Generally speaking this seems a difficult task, because the differences in core/cone altitudes derived using  $\Delta_{cc}$  are much larger than the individual values derived by other methods, see e.g., HX, R4 and R6. HX use the BCW method while R4 and R6 use pulse widths. As we discuss later the altitudes derived using the BCW offset would require a reanalysis of data for a meaningful comparison with  $\Delta r$  derived here. Before this comparison a similar and refined reanalysis for deriving better  $\Delta_{cc}$  values will also be needed.

The altitudes derived from pulse widths in R4, R6 however can be increased while maintaining the agreement with observed pulse widths. Since in the dipole geometry the cap radius  $\rho$  scales along a given flux tube with the altitude  $r$  as  $\sqrt{r}$ , an increased altitude can still lead to the same pulse width if one assumes that instead of the full emission caps, only parts of them give out radiation. This allows one to reconcile the altitudes based on pulse widths with our altitude difference.

### 5.2.1 The 1/3 rule and the filling factors

For this purpose, we introduce a simple empirical relation between core and conal widths which should be looked upon as a rule of thumb rather than a precise formula. Taking triple profiles as typical indicators of widths of the core and two conal components in one pulse, we take each one to occupy 1/3 of the total pulse width. This 'one-third' rule which has an observational origin will be seen to be of great utility and can be formalized as follows.

The core component is emitted from an altitude  $r_{core}$  where the full emission cap has the Goldreich-Julian angular radius  $\rho_{core}$ . If only a central part of the cap is emitting we describe it with a filling factor  $f_{core}$  in terms of the radius (or equivalently the pulse longitude), and it is the ratio of the radius of the part

which emits to  $\rho_{core}$ . The width of the core component is

$$W_{core} = 2 f_{core} \rho_{core}. \quad (21)$$

The conal component similarly comes from an altitude  $r_{cone}$  and a cap of Goldreich-Julian radius  $\rho_{cone}$ , but has a hollow cone. Its filling factor is  $f_{cone}$ , the ratio of the difference of the outer and inner radii of the emission region to  $\rho_{cone}$ . The width of each conal component is

$$W_{cone} = f_{cone} \rho_{cone}. \quad (22)$$

Now the 1/3 rule tells us that

$$W_{core} = W_{cone} \quad (23)$$

and invoking the  $\sqrt{r}$  scaling of  $\rho$ , we get the cone/core altitude ratio as

$$r_{cone}/r_{core} = [\rho_{cone}/\rho_{core}]^2 = 4 f_{core}^2 / f_{cone}^2 \quad (24)$$

Maximum value of  $f_{core}$  is 1 when the core emission occurs in the full cap. For  $f_{cone}$  the maximum is 2/3 and then the conal emission uniformly occupies the annulus between radii  $\rho_{cone}/3$  and  $\rho_{cone}$ . These maximum filling factors give  $r_{cone}/r_{core} = 9$ . The observed pulse widths will of course be usually less than  $W$  above due to the impact angle  $\beta$  not being zero. To stay independent of the fortuitous value of  $\beta$  which obtains for any observed pulsar, we base our discussion on  $\rho$  values alone.

*Introduction of filling factors may appear as an unwarranted additional complication, but as Eq. 24 shows, they cannot be separated from the discussion of emission altitudes.* For example the work by Rankin (R4, R6) tacitly assumes that  $f_{core}$  and  $f_{cone}$  have their maximum values of 1 and 2/3 respectively. This by the 1/3 rule would give  $r_{core}/r_{cone} = 1/9$ . Rankin's analysis is based on pulse widths and is more refined than '1/3' thumb rule, and gives  $r_{core} = R_*$  and  $r_{cone} \cong 10R_*$  (We ignore the further subtleties of inner and outer cones). Therefore the 1/3 rule captures in a simple manner the core-cone width relation and at the same time brings into focus the filling factors.

The altitudes derived by HX make use of the BCW offset and give  $r_{core} \cong 21 \pm 18 R_*$  and  $r_{cone} \cong 42 \pm 20 R_*$ . These altitudes are determined independent of any assumption about the filling factors, but in conjunction with the 1/3 rule (see Eq. 24) imply that the filling factors do not have their maximum values, in fact the mean values of altitudes imply a ratio of filling factors  $f_{core}/f_{cone} = 1/\sqrt{2}$ .

We now reconsider in turn pulsar examples in which the core component lags, has zero offset and leads respectively.

### 5.2.2 Lags

Returning now to the pulsars PSR 0329+54 and PSR 1913+16 which show lags, for altitude differences using the  $\Delta_{cc}$  we get respectively  $\Delta r \cong 115R_*$ , and  $\cong 65R_*$ , which cannot be accomodated by R4, R6 or HX.

Since altitudes derived in R4 and R6 give correct observed pulse widths, it would be desirable to maintain this. At the same time our  $\Delta r$  can also be reproduced in the following manner. If we assume a particular value for  $f_{core}/f_{cone}$  then Eq. 24 gives us the altitude ratio. Combining this with the  $\Delta r$  it is possible to derive  $r_{core}$  and  $r_{cone}$  individually, with the understanding that the higher altitude pertains to the leading component.

This way if  $f_{core}/f_{cone} = 3/2$  as in R4, R6 then  $r_{core} = 14R_*$  and  $r_{cone} = 129R_*$  for PSR 0329+54. Similarly for PSR 1913+16 we get  $r_{core} = 7R_*$  and  $r_{cone} = 72R_*$ . In this way  $\Delta_{cc}$  and R4, R6 can be reconciled.

For PSR 0329+54 the altitude quoted in HX is negative while PSR 1913+16 does not occur in their list. Also the altitude ratio  $r_{cone}/r_{core}$  for the general altitudes quoted by them varies between 0.6 and 20. If we take the mean value of 2 leading to  $f_{core}/f_{cone} = 1/\sqrt{2}$ , we can reconcile also  $\Delta_{cc}$  and HX. The altitudes then are  $r_{core} = 115R_*$  and  $r_{cone} = 230R_*$  for PSR 0329+54 and  $r_{core} = 63R_*$  and  $r_{cone} = 126R_*$  for PSR 1913+16. However, we do not attach any significance to this agreement and discuss it further in the summary subsection later.

At this point the intimate relation between emission altitudes and filling factors should be clear.

### 5.2.3 Zero offsets

In these cases both core and conal emissions occur at the same altitude. Then Eq. 24 implies that  $2f_{core} = f_{cone}$  and further because in this case  $\rho_{core} = \rho_{cone}$ , we have  $f_{core} + f_{cone} = 1$  and we find that  $2f_{core} = f_{cone} = 2/3$ . Apart from the information that their difference is zero, however, the altitudes can not be fixed any further even by using the 1/3 rule. The  $\Delta_{cc}$  corresponding to altitude differences in R4, R6 ( $\cong 10R_*$ ) or HX ( $\cong 20R_*$ ) would be small enough to agree with the observed ones. Consequently, unless the data is extremely precise the ratio  $f_{core}/f_{cone}$  is not determined, e. g., no choice can be made among either 3/2,  $1/\sqrt{2}$  or 1/2.

For zero offset cases when  $\alpha \cong 30^\circ - 50^\circ$  range, due to the multivaluedness of  $r$  an infinite number of pairs of  $r_{core}$  and  $r_{cone}$  give the same  $\Delta_{cc}$ . But if either  $r_{core}$  or  $r_{cone}$  is found to be on the rising branch (say by using BCW) and such that its  $\Delta\varphi$  is small enough to be possible only at one altitude (multivaluedness is avoided) then core and conal altitudes must lie close.

### 5.2.4 Leads

Consider the pulsars PSR 1917+00 and PSR 2028+22 for which  $\Delta_{cc}$  respectively gives  $\Delta r$  as  $\cong 60 R_*$  and  $\cong 100 R_*$ . It is obvious that altitudes given by R4, R6 or HX are of no help here because they can not give the correct sign of  $\Delta_{cc}$ .

We thus try to find  $f_{core}/f_{cone}$  in these cases using the 1/3 rule. Assuming minimum possible altitude for the conal component, i.e.,  $1 R_*$ , and using Eqs. 21 and 22 for these two pulsars we find  $f_{core}/f_{cone} = 1/16$  for PSR 1917+00 and  $1/20$  for PSR 2028+22. (The solid angle filling factors will be squares of these.) Other combinations consistent with  $\Delta_{cc}$  values will give higher altitudes and further reduce this ratio. *Unlike the cases of lags or zero offsets here clearly the full open flux tube must have large regions which do not radiate at all.*

### 5.2.5 Summary

In the above discussion of lags, leads and zero offset cases we have tried to reconcile the various altitude estimates provided the core/cone distinction is not ignored.

Intrinsically the BCW method is an excellent method for altitude determination and enjoys the advantages that use of  $\Delta_{cc}$  also entails. In both BCW and HX a puzzling feature is that the derived altitudes have large uncertainties despite having quality data and improved physics. Also in some pulsars the BCW offsets come out with a wrong sign (BCW, HX). We feel that this may be a consequence of an insufficient disentangling of core and conal features. For example, in BCW the position angle curve is dominated by the conal wings while the intensity profile is dominated by the central core in some pulsars. The BCW method as also used by HX utilises the linear polarization position angle sweep, a typical conal property, despite the reference to pulsars as 'core-dominated' etc. The position angle sweeps for cores are well known to be usually not so clean. It seems that BCW offsets in effect lead to altitudes only of conal components but in cases where the core is or is not seen. Therefore, for core components using the circular polarization signatures may provide the way. Though there is some overlap in their and our pulsar lists, the reconciliation of altitude values quoted for specific pulsars by either BCW or HX with our  $\Delta r$  here will not be meaningful; certainly so if we use  $f_{core}/f_{cone} = 1/\sqrt{2}$  which relates only to mean values of altitudes in BCW or HX. A case by case analysis can be done, but it may not prove of much value, because our  $\Delta r$  can be determined precisely only when the core and conal components have been completely separated. Therefore, it is difficult to compare our  $\Delta r$  with altitudes derived using the BCW method if the core/cone are not fully disentangled.

The considerations using pulse widths tacitly need an assumption about the filling factors. What has emerged here is that the filling factors of core/conal emissions form an integral part of the discussion and an appropriate filling factor ratio can bring about an agreement between  $\Delta r$  here and the altitudes derived

using pulse width data. Since this has been brought about by considerations of  $\Delta_{cc}$ , we see that explanation of core/cone offsets by kinematic effects has implications for the emission mechanism. Below we show that some knowledge of these filling factors can be gained if we use the 1/3 rule, further demonstrating its utility.

### 5.2.6 Variation of filling factors with altitudes

Though only the emission mechanism can provide the knowledge of filling factors it is possible to infer about one aspect of them from  $\Delta_{cc}$ . The variety in values of  $\Delta_{cc}$  most probably reflects different values of  $P$ ,  $\alpha$  and  $\beta$  for different pulsars. Imagine now pulsars arranged in an order such that successively  $\Delta_{cc}$  decreases starting from a zero value. For the zero offset case we have  $r_{core} = r_{cone}$ ,  $2f_{core} = f_{cone} = 2/3$ . Thus  $r_{cone}/r_{core} = 1$  and  $f_{cone}/f_{core} = 2$ . Now let the cone move up relative to the core. Combined with the 1/3 rule we see that this is equivalent to effectively keeping  $f_{cone} = 2/3$  and increasing  $f_{core}$  to a value  $> 1/3$ . Thus as  $\Delta_{cc}$  becomes more negative the ratio  $f_{cone}/f_{core}$  decreases as  $r_{cone}/r_{core}$  increases. Similarly we now imagine a progression of pulsars starting from zero offset and increasing  $\Delta_{cc}$ . In this case same reasoning tells us that cone is moving down relative to the core and at the same time the ratio  $f_{cone}/f_{core}$  is increasing from a starting value of 2 as  $r_{cone}/r_{core}$  decreases. Thus an important conclusion follows : *qualitatively we find that the ratio  $f_{cone}/f_{core}$  is a monotonically decreasing function of the altitude ratio  $r_{cone}/r_{core}$* . It should be noted that this filling factor variation with altitude would hold at all emission frequencies.

## 6 Conclusions

By attributing the longitude offsets between the centers of core and conal components to kinematical effects due to their having different altitudes of emission leads to the following :

- The combined offset due to aberration and *mfs* always advances the arrival time for all altitudes and inclination angles  $\alpha$ .
- Core emission does not necessarily come from the stellar surface.
- Core emission altitudes,  $r_{core}$  may be smaller, larger than or same as  $r_{cone}$ , the conal ones.
- For most pulsars  $|r_{core} - r_{cone}|$  is small compared to  $r_L$  but not necessarily compared to  $R_*$ . Indeed  $|r_{core} - r_{cone}|$  is usually much larger than the individual altitudes ascribed to core and conal components so far.

- For some pulsars  $|r_{core} - r_{cone}|$  could be comparable to  $r_L$ . This may resolve the mystery of main pulse-interpulse separations being much different from the expected  $180^\circ$ .
- Both core and conal emissions do not come from the full available part of the polar flux tube and their filling factors vary with the altitudes.

We do not wish to be more quantitative about the emission altitudes at this stage for two reasons. Firstly, on account of the previously mentioned limitations of the *mfs* formula we need a refinement in it. This should treat the sweepback more precisely using the Deutsch solution for the magnetic field of an oblique rotator and we intend to report on it soon. Secondly, the offset translates only into a difference between emission altitudes of the two components. It can determine individual altitudes only if at least one of the altitudes (core or cone) is known definitely.

In the foregoing we have ignored the possible contributions to phase offsets by the emission mechanism(s). Can emission mechanisms contribute significantly to the phase offset of a pulse component? Note firstly that aberration and the 'mfs' are first order effects. As seen in Figs. 1 and 2, these offsets are individually quite large over most of the range of  $v$  as well as  $\alpha$ . Similarly from Figs. 3 and 4, the same is true even when we deal with their difference, i.e.,  $\Delta\varphi$ . Even at small (but not extremely small) values of  $v$ , and, also  $\alpha$ , the net offset is significant. For the emission mechanism to affect this, its contribution should also be equally significant. If this is true then our considerations would need modifications.

On the other hand, irrespective of these dynamical contributions which are also not known, the effects considered by us must be present. From the foregoing there is ample indication that they suffice for describing the observed core/cone longitude offsets coming into play due to the emission mechanism selecting different altitudes of emission, perhaps strongly varying with period, inclination angle etc. In addition, they are providing constraints on the emission mechanisms, e.g., the unexpectedly small filling factors for the core components for those pulsars in which core leads.

Now, we briefly comment on multifrequency observations. As the frequency of observation decreases,  $\Delta_{ec}$  remains negative but increases in magnitude for some pulsars (e.g., PSR 0329+54, see, e.g., Malov and Suleimanova 1998) while it decreases to such an extent that it changes from negative to positive for PSR 1821+05 (see, e.g., Weisberg et al. 1999). Since our considerations bring in filling factor variations, both frequency and geometry of emission change with the altitude. Thus, our picture potentially can explain the otherwise perplexing observations and its application will lead to very insightful constraints on the emission mechanism. In addition, *a rfm opposite of the conventional one is also a possibility*. This seems to have been observed by Rankin (2001, private communication).

The full predictive potential of our framework can be realized if it is combined with a detailed analysis of morphological, polarization and multifrequency observations. We offer one concrete suggestion in this connection.

The total intensity profile of a pulsar could be separated into individual Gaussian components. The circular polarization signature could be used to identify the core component. A precise determination of the above offset will then immediately lead to an altitude difference. A polarization position angle curve for each component can be constructed using the rotating vector model and known  $\alpha$  and  $\beta$  values. A composite of these which reproduces the observed position angle curve can be constructed. Then the BCW offsets between intensity and the position angle curve centroids for each component will allow determination of individual altitudes. It may be noted that the BCW offsets can be unambiguously determined only if position angle sweeps are clean, which typically occurs for conal components. (If BCW method is applied and very large altitudes are considered, then its modification to include *mfs* will be needed). With the thus obtained conal altitude combined with  $\Delta_{cc}$  the core altitude can be fixed. The filling factors can then be determined by the 1/3 rule proposed here. Consistency of this information with multifrequency observations will permit a further look into issues like radius to frequency mapping, time delays etc.

We hope to have demonstrated in previous sections that the kinematical effects considered here have the potential to explain the core/cone longitude offsets and also shed light on the nature of the emission mechanism, and therefore a detailed observational study of these offsets holds much promise in elucidating the intricacies of pulsar emission.

## References

- [1] Blaskiewicz, M., Cordes, J.M., & Wasserman, I. 1991, ApJ **370**, 643 (BCW)
- [2] Cordes, J. M. 1992, The Magnetospheric Structure and Emission Mechanisms of Radio Pulsars (Eds. Rankin et al.), Pedagogical University Press, p. 253.
- [3] Cordes, J. M., Rankin, J. M. & Backer, D. C. 1978, ApJ **223**, 961
- [4] Cordes, J. M., Wasserman, I. & Blaskiewicz, M. 1990, ApJ **349**, 546
- [5] Deutsch, A.J. 1955, Ann. d'Astrophysique **18**, 1
- [6] Gangadhara, R.T. & Gupta, Y. 2001, ApJ **555**, 31
- [7] Goldreich, P. & Julian, W.H. 1969, ApJ **157**, 869
- [8] Hankins, T.H. & Rickett, B.J. 1986, ApJ **311**, 684

- [9] Hirotani, K. 2000, MNRAS **317**, 225
- [10] von Hoensbroech, A. & Xilouris, K M 1997, A & A **324**, 981 (**HX**)
- [11] Kapoor, R. C. & Shukre, C.S. 1998, ApJ **501**, 228 (**KS**)
- [12] Kapoor, R. C. & Shukre, C. S. 1999, Bulletin Astron Soc. India **27**, 207
- [13] Kapoor, R. C. & Shukre, C.S. 2001, A & A **372**, 405
- [14] Kijak, J. & Gil, J. 1998, MNRAS **299**, 855.
- [15] Kuzmin, A.D., Izvekova, V.A., Shitov, Yu.P., Sieber, W., Jessner, A., Wielebinski, R., Lyne, A.G. & Smith, F.G. 1998, A & A Suppl. **127**, 355
- [16] Lyne, A. G. & Manchester, R. N. 1988, MNRAS **234**, 477 (**LM88**)
- [17] Lyne, A.G., Smith, F.G., & Graham, D.A. 1971, MNRAS **153**, 337
- [18] Malov I. F. & Suleimanova S. A. 1998, Astron. Reports **42**, 388
- [19] Manchester, R. N. , Hamilton, P.A. & McCulloch, P.M. 1980, MNRAS **192**, 153
- [20] McCulloch, P. M., Hamilton, P. A. , Ables, J. G., & Komessaroff, M. M. 1976, MNRAS **175**, 71p
- [21] Nowakowski,L.A., 1994, A &A **281**, 444
- [22] Philips, J.A. 1992, ApJ **385**, 282
- [23] Rankin, J. 1983, ApJ **274**, 359 (**R1**)
- [24] Rankin, J. 1986, ApJ **301**, 901 (**R3**)
- [25] Rankin, J. 1990, ApJ **352**, 247 (**R4**)
- [26] Rankin, J. 1993, ApJ **405**, 285 (**R6**)
- [27] Rankin, J., Stinebring, D.R.,& Wiesberg, J.M. 1989, ApJ **346**, 869 (**RSW89**)
- [28] Seiradakis, J.H., Gil, J.A., Graham, D.A., Jessner, A., Kramer, M.,Malofeev, V.M., Sieber, W., & Wielebinski, R. 1995, A &A Suppl. **111**, 205
- [29] Shitov, Yu. P. 1983, Soviet Astron. **27**, 314
- [30] Shitov, Yu. P. 1985, Soviet Astron. **29**, 33
- [31] Sieber, W., Reinecke, R. & Wielebinski, R. 1975, A & A **38**, 169

- [32] Weisberg, J.M., Armstrong, B.K., Backus, P.R., Cordes, J.M., Boriakoff, V. & Ferguson, D.C. 1986, *Astron. J.* **92**, 621
- [33] Weisberg, J.M., Cordes, J.M., Lundgren, S.C., Dawson, B.R., Despotes, J.T., Morgan, J.J., Weitz, K.A., Zink, E.C., & Backer, D.C., 1999, *ApJS* **121**, 171
- [34] Xilouris, K M, Rankin, J, Seiradakis, J H ,& Sieber W, 1991, *A & A* **241**, 87

Table 1: Phase offsets for some pulsars

SN	Pulsar	Type	$\Delta_{cc}$ (deg.)	P (s)	$\alpha$ (deg.)	$\beta$ (deg.)	$\Delta r$ $R_*$	$\Delta v$
1	0329+54	T	-2.0 <sup>a</sup>	0.715	30.8	+2.9	120	0.017
2	0450-18	T	0.0 <sup>b</sup>	0.549	31.0	+4.9	—	—
3	0523+11	T	+1.0 <sup>k</sup>	0.354	49.1	+4.6	30	0.015
4	1451-68	T	0.0 <sup>b</sup>	0.263	23.5	+3.3	—	—
5	1700-32	T	0.0 <sup>b</sup>	1.212	47.0	+1.7	—	—
6	1804-08	T	0.0 <sup>c</sup>	0.164	46.7	+2.0	—	—
7	1821+05	T	-1.9 <sup>d</sup>	0.753	32.0	-1.5	118	0.018
8	1826-17	T	-1.5 <sup>c</sup>	0.307	39.6	+0.7	40	0.018
9	1913+16	T	-12.0 <sup>l</sup>	0.059	46.0	+1.0	60	0.160
10	1917+00	T	+0.6 <sup>e</sup>	1.27	78.2	-1.2	62	0.010
11	1926+18	T	+0.6 <sup>d</sup>	1.221	35.0	-	66	0.006
12	1933+16	T	-0.5 <sup>f</sup>	0.359	64.9	+1.0	16	0.008
13	1946+35	T	0.0 <sup>b</sup>	0.717	43.1	+4.4	—	—
14	2045-16	T	-2.1 <sup>b</sup>	1.96	37.0	+1.1	330	0.022
15	2111+46	T	-3.6 <sup>g</sup>	1.015	8.6	+1.3	320	0.010
16	2319+60	T	0.0 <sup>b</sup>	2.256	19.0	+2.3	—	—
17	1237+25	M	-1.3 <sup>h</sup>	1.382	53.0	-0.9	200	0.025
18	1737+13	M	-0.8 <sup>i</sup>	0.803	41.0	-2.5	52	0.009
19	1857-26	M	-1.6 <sup>b</sup>	0.612	21.0	-1.6	81	0.010
20	2028+22	M/T	+1.9 <sup>j</sup>	0.631	50.0	+5.5	105	0.025

References from where the  $\Delta_{cc}$  value is obtained:

- a - Lyne et al. (1971); b - LM88; c - Seiradakis et al. (1995);  
d - Weisberg et al. (1986); e - RSW89; f - Sieber et al. (1975);  
g - Kuzmin et al. (1998); h - R1; i - Blaskiewicz et al. (1990);  
j - Hankins and Rickett (1986); k - Weisberg et al. (1999);  
l - Cordes et al. (1990).

Table 2: Large phase offsets cases

SN	Pulsar	Type	$\Delta_{cc}$ (deg.)	P (s)	$\alpha$ (deg.)	$\beta$ (deg.)	$\Delta r$ $R_*$	$\Delta v$
1	1802+03	—	$\leq +4.1$	0.219	—	—	75	$\leq 0.07$
2	1822-09	$T_{1/2}$	$\leq -7.5$	0.789	86.0	+1.1	490	0.130
3	1842+14	$T/S_t$	$\leq +3.9$	0.375	63.0	+4.2	125	0.063
4	1859+03	$S_t/T_{1/2}$	$\leq -5.6$	0.655	38.7	+3.6	310	0.063
5	1907+10	$S_t$	$\leq -3.8$	0.284	90.0	—	91	0.067
6	1920+21	T	$\leq +4.5$	1.078	47.0	+1.2	420	0.060
7	2020+28	T	$\leq +5$	0.343	71.0	+3.6	145	0.080
8	2224+65	$T_{1/2}$	$\leq +15$	0.683	16.0	+3.4	900	0.080
9	0531+21	$T_{1/2}$	+22	0.033	90.0	—	100	0.650
10	0823+26	$T_{1/2}$	+30	0.531	90.0	—	2480	0.980
11	1055-52	T	+16	0.197	90.0	0.0	300	0.330
12	1742-30	T	-9	0.367	57.0	—	290	0.140